Asymmetric femtosecond laser ablation of silicon surface governed by the evolution of surface nanostructures

Cheng-Yun Zhang,[1,2] Jian-Wu Yao,[1] Chang-Qing Li,[1] Qiao-Feng Dai,[1] Sheng Lan,[1,*] Vyacheslav A. Trofimov,[3] and Tatiana M. Lysak[3]

[1]*Laboratory of Nanophotonic Functional Materials and Devices, School of Information and Optoelectronic Science and Engineering, South China Normal University, Guangzhou 510006, China*
[2]*School of Physics and Electronic Engineering, Guangzhou University, Guangzhou 510006, China*
[3]*Department of Computational Mathematics and Cybernetics, M. V. Lomonosov Moscow State University, Moscow 119992, Russia*
[*]*slan@scnu.edu.cn*

Abstract: The femtosecond laser ablation of silicon surface near the ablation threshold was investigated and the preferential ablation along different directions was observed in different stages. It was found that the ripples formed in the initial stage facilitate the ablation along the direction perpendicular to the ripples, leading to the formation of an elliptical ablation area. With increasing length and depth of the ripples, however, nanohole arrays formed in the ripples will modify the distribution of electric field which benefits the ablation along the direction parallel to the ripples. Consequently, the ablation area is gradually changed to a circular one after irradiating sufficient number of pulses.

OCIS codes: (220.4241) Nanostructure fabrication; (350.3390) Laser materials processing; (320.7090) Ultrafast lasers.

References and links

1. B. Dusser, Z. Sagan, H. Soder, N. Faure, J. P. Colombier, M. Jourlin, and E. Audouard, "Controlled nanostructrures formation by ultra fast laser pulses for color marking," Opt. Express **18**(3), 2913–2924 (2010).
2. A. Y. Vorobyev and C. Guo, "Femtosecond laser nanostructuring of metals," Opt. Express **14**(6), 2164–2169 (2006).
3. A. Y. Vorobyev and C. Guo, "Colorizing metals with femtosecond laser pulses," Appl. Phys. Lett. **92**(4), 041914 (2008).
4. C. A. Zuhlke, D. R. Alexander, J. C. Bruce 3rd, N. J. Ianno, C. A. Kamler, and W. Yang, "Self assembled nanoparticle aggregates from line focused femtosecond laser ablation," Opt. Express **18**(5), 4329–4339 (2010).
5. L. Qi, K. Nishii, and Y. Namba, "Regular subwavelength surface structures induced by femtosecond laser pulses on stainless steel," Opt. Lett. **34**(12), 1846–1848 (2009).
6. I. Umezu, Y. Nakayama, and A. Sugimura, "Formation of core-shell structured silicon nanoparticles during pulsed laser ablation," J. Appl. Phys. **107**(9), 094318 (2010).
7. M. Beresna and P. G. Kazansky, "Polarization diffraction grating produced by femtosecond laser nanostructuring in glass," Opt. Lett. **35**(10), 1662–1664 (2010).
8. M. Shen, J. E. Carey, C. H. Crouch, M. Kandyla, H. A. Stone, and E. Mazur, "High-density regular arrays of nanometer-scale rods formed on silicon surfaces via femtosecond laser irradiation in water," Nano Lett. **8**(7), 2087–2091 (2008).
9. X. Jia, T. Q. Jia, Y. Zhang, P. X. Xiong, D. H. Feng, Z. R. Sun, J. R. Qiu, and Z. Z. Xu, "Periodic nanoripples in the surface and subsurface layers in ZnO irradiated by femtosecond laser pulses," Opt. Lett. **35**(8), 1248–1250 (2010).
10. M. Huang, F. Zhao, Y. Cheng, N. Xu, and Z. Xu, "Origin of laser-induced near-subwavelength ripples: interference between surface plasmons and incident laser," ACS Nano **3**(12), 4062–4070 (2009).
11. J. E. Sipe, J. F. Young, J. S. Preston, and H. M. van Driel, "Laser-induced periodic surface structure. I. Theory," Phys. Rev. B **27**(2), 1141–1154 (1983).
12. S. Sakabe, M. Hashida, S. Tokita, S. Namba, and K. Okamuro, "Mechanism for self-formation of periodic grating structures on a metal surface by a femtosecond laser pulse," Phys. Rev. B **79**(3), 033409 (2009).
13. T. Q. Jia, H. X. Chen, M. Huang, F. L. Zhao, J. R. Qiu, R. X. Li, Z. Z. Xu, X. K. He, J. Zhang, and H. Kuroda, "Formation of nanogratings on the surface of a ZnSe crystal irradiated by femtosecond laser pulses," Phys. Rev. B **72**(12), 125429 (2005).

#179706 - $15.00 USD Received 15 Nov 2012; revised 23 Jan 2013; accepted 7 Feb 2013; published 13 Feb 2013

14. A. Y. Vorobyev, V. S. Makin, and C. Guo, "Periodic ordering of random surface nanostructures induced by femtosecond laser pulses on metals," J. Appl. Phys. **101**(3), 034903 (2007).
15. Q. Sun, F. Liang, R. Vallée, and S. L. Chin, "Nanograting formation on the surface of silica glass by scanning focused femtosecond laser pulses," Opt. Lett. **33**(22), 2713–2715 (2008).
16. Y. Shimotsuma, P. G. Kazansky, J. Qiu, and K. Hirao, "Self-organized nanogratings in glass irradiated by ultrashort light pulses," Phys. Rev. Lett. **91**(24), 247405 (2003).
17. V. R. Bhardwaj, E. Simova, P. P. Rajeev, C. Hnatovsky, R. S. Taylor, D. M. Rayner, and P. B. Corkum, "Optically produced arrays of planar nanostructures inside fused silica," Phys. Rev. Lett. **96**(5), 057404 (2006).
18. F. Liang, R. Vallée, and S. L. Chin, "Mechanism of nanograting formation on the surface of fused silica," Opt. Express **20**(4), 4389–4396 (2012).
19. D. Dufft, A. Rosenfeld, S. K. Das, R. Grunwald, and J. Bonse, "Femtosecond laser-induced periodic surface structures revisited: A comparative study on ZnO," J. Appl. Phys. **105**(3), 034908 (2009).
20. J. W. Yao, C. Y. Zhang, H. Y. Liu, Q. F. Dai, L. J. Wu, S. Lan, A. V. Gopal, V. A. Trofimov, and T. M. Lysak, "High spatial frequency periodic structures induced on metal surface by femtosecond laser pulses," Opt. Express **20**(2), 905–911 (2012).
21. J. Bonse, M. Munz, and H. Sturm, "Structure formation on the surface of indium phosphide irradiated by femtosecond laser pulses," J. Appl. Phys. **97**(1), 013538 (2005).
22. C. Y. Zhang, J. W. Yao, H. Y. Liu, Q. F. Dai, L. J. Wu, S. Lan, V. A. Trofimov, and T. M. Lysak, "Colorizing silicon surface with regular nanohole arrays induced by femtosecond laser pulses," Opt. Lett. **37**(6), 1106–1108 (2012).
23. J. Bonse, A. Rosenfeld, and J. Krüger, "On the role of surface plasmon polaritons in the formation of laser-induced periodic surface structures upon irradiation of silicon by femtosecond-laser pulses," J. Appl. Phys. **106**(10), 104910 (2009).
24. J. Bonse, A. Rosenfeld, and J. Krüger, "Implications of transient changes of optical and surface properties of solids during femtosecond laser pulse irradiation to the formation of laser-induced periodic surface structures," Appl. Surf. Sci. **257**(12), 5420–5423 (2011).
25. G. Obara, N. Maeda, T. Miyanishi, M. Terakawa, N. N. Nedyalkov, and M. Obara, "Plasmonic and Mie scattering control of far-field interference for regular ripple formation on various material substrates," Opt. Express **19**(20), 19093–19103 (2011).

1. Introduction

Femtosecond (fs) laser ablation has attracted great interest in the last two decades because of its capability in the fabrication of micro- and nanostructures (including micro- and nanoparticles) which may find potential applications in various fields of science and technology [1–4]. For the creation of micro- and nanostructures on the surfaces of different materials [3,5–9], laser fluence near or just above the ablation threshold of the material is usually adopted and much effort has been devoted to the study of the micro- or nanostructures generated in this situation. Although the underlying physical mechanism responsible for the formation of laser-induced periodic surface structures (LIPSSs) or ripples remains controversial [10–15], it is generally suggested that the interference between the excited surface plasmon wave (or scattered wave) with the incident light plays a crucial role in the formation of such kind of ripples [10,11,14]. Other physical mechanisms that have been proposed to interpret the formation of LIPSSs and nanogratings include the interference between the incident light field and the electric field of bulk electron plasma wave [16], local field enhancement [17] and the incubation effect [18]. It implies that the ablation is generally dominated by the distribution of electric field on the surface of the material. In recent years, LIPSSs with deep subwavelength periods were observed and different mechanisms have been proposed to interpret the formation of these high spatial frequency LIPSSs [19–21]. Very recently, we have demonstrated the colorizing of silicon surface with one-dimensional (1D) nanohole chains or two-dimensional (2D) nanohole arrays [22]. Physically, the formation of high spatial frequency LIPSSs and nanohole arrays can be successfully explained by the redistribution of electric field induced by the initially formed ripples (or low spatial frequency LIPSSs) [20,22].

In this article, we investigate the evolution of the micro- and nanostructures induced on silicon surface with increasing number of fs laser pulses with laser fluence near the ablation threshold. It is found that the redistribution of electric field leads to the preferential ablation along different directions in different stages. The preferential ablation along the direction perpendicular to the ripples in the initial stage is gradually changed to the direction parallel to the ripples due to the redistribution of electric field. As a result, the elliptical ablation area

#179706 - $15.00 USD Received 15 Nov 2012; revised 23 Jan 2013; accepted 7 Feb 2013; published 13 Feb 2013

observed in the initial stage evolves gradually into a circular one with increasing number of irradiating pulses.

2. Experimental details

In experiments, micro- and nanostructures were produced on the surface of a n-doped silicon wafer by using the 800-nm laser pulses delivered by a fs amplifier (Legend, Coherent). The duration and repetition rate of the laser pulses are 100 fs and 1 kHz, respectively. The resistivity of the silicon wafer is smaller than 0.01 Ω cm. The surface orientation is (100) and the surface roughness is less than 0.5 nm. The laser beam with a diameter of 5.1 mm defined by a diaphragm and a Gaussian profile was focused normally on the surface of the silicon wafer by using a lens with a focusing length of 150 mm, producing an excitation spot of ~40 μm in diameter. The laser fluence was adjusted by using the combination of a waveplate and a polarizer. The ablation was carried out in air by irradiating the focused spot with different numbers of pulses controlled by a mechanical gate connected to a computer. The morphology of the silicon surface after fs ablation was examined by using scanning electron microscope (SEM). After the formation of initial ripples, it is expected that the interaction of laser with material surface would be changed, leading to the redistribution of the incident laser that may significantly affect the subsequent ablation process. It has been shown that the initially formed ripples, which behave as a surface grating, will facilitate the coupling between the incident laser light and the surface plasmon wave [10,14,23]. In this case, a further deepening of the ripples is anticipated, resulting in deep grooves on the surface where the incident light is strongly localized.

3. Results and discussion

3.1 Asymmetric ablation observed on silicon surface

The SEM images of the nanostructures formed on the silicon surface with increasing pulse number (N) are presented in Fig. 1. The polarization of the laser light was horizontal and the laser fluence was chosen to be 148 mJ/cm^2. For N = 5, one can see ripples with a subwavelength period (~720 nm) aligned in the vertical direction which is perpendicular to the polarization of the laser light. The ablation was observed to occur in a circular area with a diameter of ~7.8 μm. However, it was found that the ripples were formed in a rectangular area of 7.8 × 3.9 μm^2, as indicated in Fig. 1(a). When N was increased to 25, the length of the rectangular area decorated with ripples was increased to ~15 μm while its width remained nearly unchanged. In addition, it was noticed that two rows of nanoholes with a separation of ~2 μm were created in the ripples. As N became 35, no further development of the ablation region was observed in the horizontal direction. In contrast, the ablation region in the vertical direction was increased to ~6 μm as shown in Fig. 1(c). From N = 35 to N = 55, the ablation occurred only in the vertical direction and the elliptical ablation area eventually became a circular one decorated with 2D nanohole arrays at N = 55.

For laser fluence near the ablation threshold, the ablation process proceeds in several stages with increasing pulse number. In the first stage, ripples with a subwavelength period are formed due to the interference between the excited surface plasmon wave (or scattered wave) with the incident light. Then, the incident light becomes localized in the ripples [10], leading to the elongation and deepening of the ripples. During this stage, a redistribution of electric field induced by the initially formed ripples occurs, resulting in the extension of electric field distribution in the direction perpendicular to the ripples. This phenomenon can be verified by numerical simulation which will be shown in the following. The extension of electric field leads to the preferential ablation in this direction, which is manifested in the extension of ripples and the rectangular ablation area shown in Fig. 1(a). In the third stage, nanohole arrays are created in the ripples due to the redistribution of the electric field when the length and depth of the ripples exceed critical values [22]. As a result, the light is localized in the nanoholes, resulting in the redistribution of electric field. In the final stage, the redistribution of electric field caused by the nanohole arrays facilitates the ablation in the

#179706 - $15.00 USD Received 15 Nov 2012; revised 23 Jan 2013; accepted 7 Feb 2013; published 13 Feb 2013

direction parallel to the ripples and the elliptical ablation area is gradually changed to a circular one.

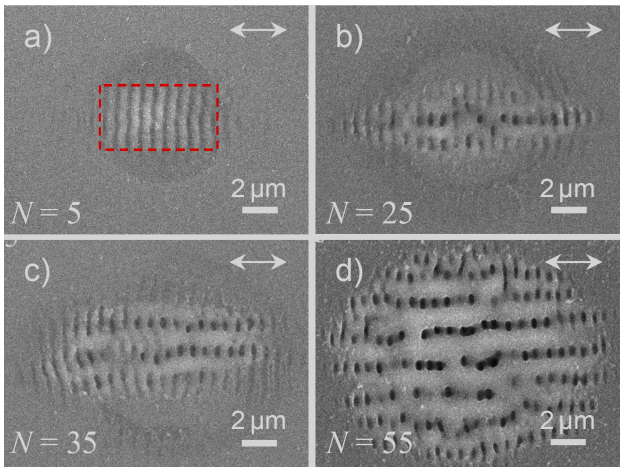

Fig. 1. Evolution of the nanostructures induced on the surface of the silicon wafer with increasing pulse number showing asymmetric ablation. (a) N = 5, (b) N = 25, (c) N = 35, and (d) N = 55. The laser light is horizontally polarized. The rectangle in (a) shows the ablation area where ripples are formed.

3.2 Numerical simulation of electric field distribution based on the FDTD technique

In order to gain a deep insight into the effect of electric field redistribution on the ablation, we have calculated the electric field distribution on the surface of the silicon wafer and its evolution with the formation of various nanostructures by using the finite-difference time-domain (FDTD) technique, as shown in Fig. 2. In the FDTD simulation, we used a perfectly matched layer boundary condition with a reflection as small as 10^{-8}. Previously, similar method has been successfully employed to simulate the formation of nanohole arrays on silicon surface [22]. For simplicity, the physical model used to describe the ripples formed in the first stage is a silicon wafer with five initially formed grooves (ripples).

Physically, the electric field distribution will be determined by both the excited surface plasmon wave and the scattered wave. The former is induced by the high density of carriers generated by fs laser pluses while the latter is caused mainly by the surface structure. In the numerical simulations, the key issue is how to appropriately include the effects of the excited surface plasmon wave into the physical model. Actually, it has been shown that the formation of ripples will facilitate the coupling between the incident light and the surface plasmon wave [10]. In the normal state, the absorption coefficient of silicon is found to be α = 606 cm^{-1} at 800 nm, corresponding to an extinction coefficient of κ = 0.004 [22]. Under the irradiation of fs laser pulses, however, the complex refractive index of silicon would be dramatically modified due to the high density of photogenerated electrons. In this case, the dielectric constant of silicon $\varepsilon(\omega)$ can be described by the Drude model, which is expressed as [10],

$$\varepsilon(\omega) = \varepsilon_r(\omega) + i\varepsilon_i(\omega) = \varepsilon_c - \frac{\omega_p^2}{\omega(\omega + i\Gamma)} \tag{1}$$

where ε_c is the dielectric constant in the normal state, $\omega_p = [e^2 n_e/(m_{eff}\varepsilon_0)]1/2$ is the plasma frequency, and Γ is the electron collision frequency. It is noticed that ω_p can be quite large if a large carrier density n_e is produced under the irradiation of fs laser. From Eq. (1), the real and imaginary parts of the dielectric constant can be derived as follows

#179706 - $15.00 USD Received 15 Nov 2012; revised 23 Jan 2013; accepted 7 Feb 2013; published 13 Feb 2013

$$\varepsilon_r(\omega) = \varepsilon_c - \frac{\omega_p^2}{(\omega^2 + \Gamma^2)}$$
$$\varepsilon_i(\omega) = \frac{\omega_p^2 \Gamma}{\omega(\omega^2 + \Gamma^2)} \quad (2)$$

It can be seen that a significant increase in ε_i due to large ω_p is expected under the excitation of fs laser, implying a large α or κ for silicon. Theoretical studies revealed that both the real and imaginary parts of the complex refractive index depend strongly on the density of electrons, especially in the case of high electron density [24]. In addition, the carrier density range in the ablation of silicon was also estimated [19,24]. In our case, the laser fluence we used was close to the ablation threshold of silicon and the carrier density was estimated to be ~10^{21} cm^{-3}. Therefore, we chose the complex refractive index of silicon as n = 3.4 + i0.5 in the numerical simulations. It was revealed that that the large α or κ of silicon induced by fs laser irradiation plays a crucial role in localizing laser light in the grooves [22].

It has been shown that maxima of electric field begin to appear in the ripples when the length (l) and depth (h) of the grooves exceed critical values [22]. It implies the preferential ablation at the maxima of electric field and the formation of nanohole arrays. A typical example (l ~4.0 μm and h ~0.12 μm) showing the formation of two rows of nanoholes is presented in Fig. 2(b) where the extension of electric field along the direction perpendicular to the ripples is observed. It indicates the preferential ablation along this direction. In Fig. 2(a), we show the physical model employed to describe the ripples decorated with 2D nanohole arrays. Here, we assume that two rows of nanoholes have been created in the grooves, similar to the situation shown in Fig. 1(b). In order to clearly show the detailed structure, the silicon wafer has been cleaved along the central line of the third groove. The other parameters characterizing the structure include the period of the grooves (d), the separation between the two nanoholes in each groove (a), the length (c), width (t) and height (b) of the nanoholes, as depicted in the inset. In Fig. 2(c), we present the calculated electric field on the surface of the silicon by using the following parameters: d = 0.8 μm, a = 2.0 μm, c = 0.3 μm, t = 0.2 μm, and b = 0.2 μm. It can be seen that the extension of electric field in the horizontal direction remains nearly unchanged while a significant extension of electric field appears in the vertical direction. As a result, no more grooves will be formed in the horizontal direction. Instead, the grooves will become longer and deeper, resulting in the formation of more nanoholes in the grooves, as shown in Fig. 1(c). The electric field redistribution with the evolution of surface structure dominates the ablation process and explains well the change of the elliptical ablation area to a circular one with increasing pulse number. In fact, nanoparticles or nanostructures intentionally induced on the surface of a material have been employed to create electric field distributions of different types by utilizing the interference between the scattered wave and the incident light. It was shown that the interference pattern generated in this way dominated the ablation of the surface [25].

It should be emphasized that the nanohole arrays reported previously were created by scanning the laser light on the surface of silicon wafer [22]. The change in the length and depth of the grooves was caused by the increase in laser fluence. Here, the laser fluence was fixed and only the number of irradiating pulses was increased. Therefore, the increase in the length and depth of the grooves originates from the electric field redistribution from one pulse to the other. It can be easily seen in Fig. 2(c) that the maximum of laser intensity is no longer located at the centre of the laser spot after the formation of nanoholes where the light is strongly localized. Instead, it has been shifted away from the centre in the vertical direction. In Fig. 2(c), the strongest electric field appears in the nanoholes but strong electric field is also observed at Y = ± 2 μm. Since a perfectly matched layer boundary condition with a small reflection of 10^{-8} was employed in the numerical simulation, the strong electric field is caused by the formation of nanoholes and it is responsible for the preferential ablation in the

#179706 - $15.00 USD Received 15 Nov 2012; revised 23 Jan 2013; accepted 7 Feb 2013; published 13 Feb 2013

vertical direction. This phenomenon explains why the ablation is shifted to the direction parallel to the grooves.

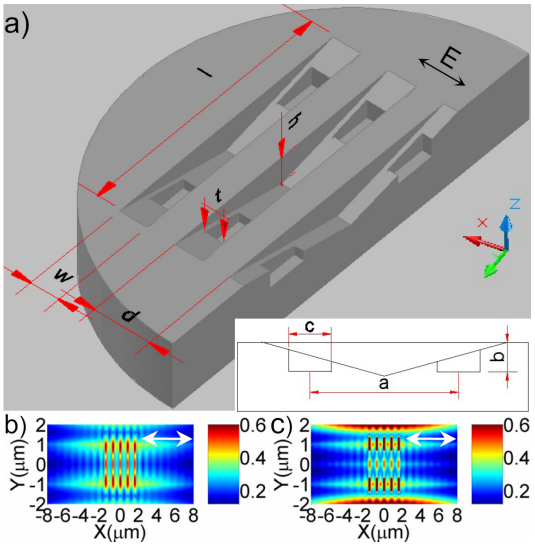

Fig. 2. (a) Schematic showing the geometry of the initially formed grooves decorated with two rows of nanoholes employed in the numerical simulation. (b) The calculated electric field distribution on the surface of the grooves whose structural parameters are chosen to be l = 4.0 μm and h = 0.12 μm. (c) The modified electric field distribution on the surface of the grooves decorated with two rows of nanoholes whose structural parameters are: d = 0.8 μm, a = 2.0 μm, c = 0.3 μm, t = 0.2 μm, and b = 0.2 μm. The fs laser light is horizontally polarized.

3.3 Asymmetric ablation observed on silicon surface along different directions

It has been known that the alignment of the ripples depends strongly on the polarization of the laser light. Similar asymmetric ablation was also observed in other directions when the laser polarization was changed although the ablation threshold may be different in different directions. The SEM images showing the evolution of the ablation with increasing pulse number for (110), (010) and (−110) directions are presented in Fig. 3. The evolution of the ablation exhibits a behavior similar to that observed in the ablation carried out in the (100) direction.

The laser fluence we used in the ablation experiments (148 mJ/cm^2) is close to the ablation threshold of silicon. Therefore, we could clearly observe the formation of ripples and nanohole arrays and the asymmetric ablation described in this paper. Actually, we have tried to ablate silicon with a laser fluence of 296 mJ/cm^2, which is much higher than the ablation threshold of silicon. In this case, the formation of ripples and nanohole arrays was not clearly observed, so was the asymmetric ablation.

#179706 - $15.00 USD Received 15 Nov 2012; revised 23 Jan 2013; accepted 7 Feb 2013; published 13 Feb 2013

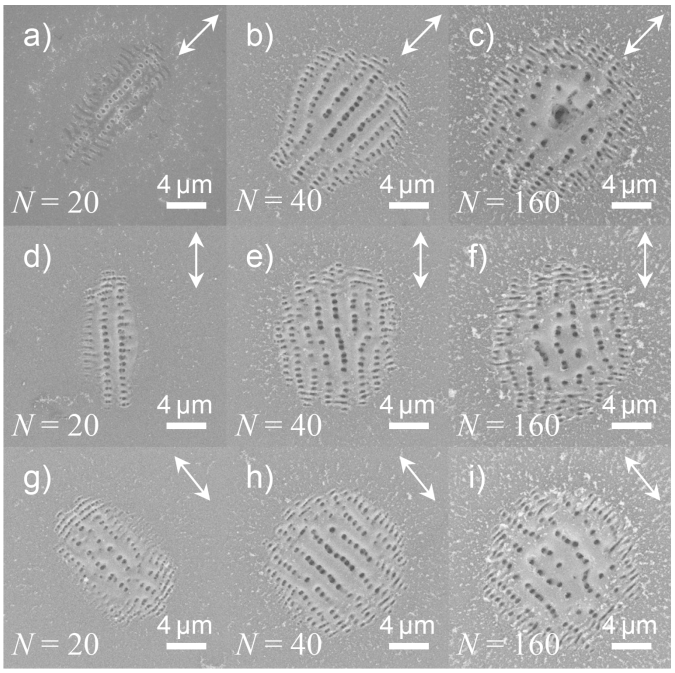

Fig. 3. Evolution of the nanostructures induced on the surface of the silicon wafer with increasing pulse number (N = 20, 40, and 160) observed in the (110), (010), and (−110) directions. The arrows indicate the polarization of the laser light.

3.4 Asymmetric ablation observed on nickel surface

In above discussion, we have suggested that the change in preferential ablation direction originates from the formation of 2D nanohole arrays and it was demonstrated by FDTD simulation. Here, we present other evidence that supports this interpretation. In Fig. 4, we show the evolution of the nanostructures ablated on the surface of a nickel foil with increasing pulse number. The laser fluence was fixed to be 148 mJ/cm^2. Due to the difference in material properties such as electronic and thermal conductivities, we did not observe the formation of 2D nanohole arrays. Instead, high spatial frequency LIPSSs with a deep subwavelength period (~267 nm) was observed. This phenomenon can also be explained by the redistribution of electric field induced by initially formed grooves with nearly constant depth within the ablation area [20]. Without the formation of 2D nanohole arrays, the change in preferential ablation direction does not occur and the ablation area remains to be elliptical even after irradiating a large number of pulses (N = 300), as shown in Fig. 4.

In the experiments described in this paper, we used the same laser fluence (148 mJ/cm^2) to ablate silicon and nickel and compared the ablation results. So far, we did ablation experiments for nickel by using only this laser fluence. However, we have tried to ablate other metals (such as stainless steel and titanium) with different laser fluences. For all the metals we have investigated, we observed only the formation of ripples (low spatial frequency LIPSSs) and high spatial frequency LIPSSs with a deep subwavelength period (see Fig. 4). The formation of nanohole arrays was not observed. Since the transition from the preferential ablation in the direction parallel to laser polarization to that in the direction perpendicular to the laser polarization is caused by the formation of nanohole arrays, such a transition has not been found in the ablation of metals.

#179706 - $15.00 USD Received 15 Nov 2012; revised 23 Jan 2013; accepted 7 Feb 2013; published 13 Feb 2013

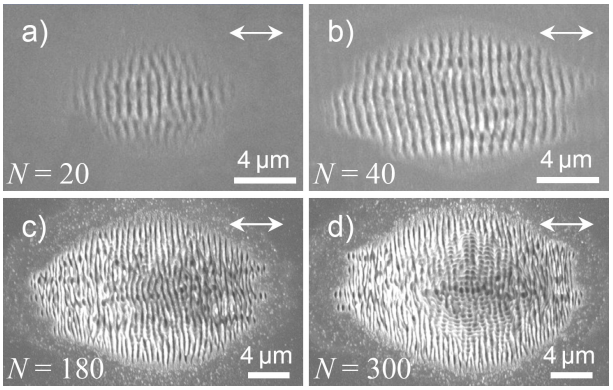

Fig. 4. Evolution of the nanostructures induced on the surface of the nickel foil with increasing pulse number showing preferential ablation only in the horizontal direction. (a) $N = 20$, (b) $N = 40$, (c) $N = 180$, and (d) N = 300. The laser light is horizontally polarized.

4. Summary

In summary, we have investigated the asymmetric ablation of silicon surface in different stages of the ablation process. The physical mechanism responsible for the asymmetric ablation is revealed to be the electric field redistribution induced by the evolution of the surface structure based on the FDTD simulation. It was found that the ablation area will eventually evolves from an elliptical shape to a circular one with increasing pulse number due to the formation of 2D nanohole arrays. This explanation is supported by the experimental observation on the ablation of nickel surface. The understanding of the physical mechanism of fs laser ablation near the threshold will be helpful for the creation of periodic micro- and nanostructures such as nanohole arrays that may find potential applications in the fields of anti-counterfeiting, color display, encryption, optical data storage, and microfluid channels.

Acknowledgments

The authors acknowledge the financial support from the National Natural Science Foundation of China (Grant Nos. 10974060, 51171066 and 11111120068), the Ministry of Education (Grant No. 20114407110002) and the program for high-level professionals in the universities of Guangdong province, China.

#179706 - $15.00 USD Received 15 Nov 2012; revised 23 Jan 2013; accepted 7 Feb 2013; published 13 Feb 2013